Fangyingnan Zhang, Xinning Wang, Xiaoqi Zhang, Saquib Waheed, Rong Zhong, Ubaldo Armato, Jun Wu, Anna Chiarini, Ilaria Dal Prà, Chao Zhang* and Zhibin Li*

Human EVI2B acts as a Janus-faced oncogene/antioncogene by differently affecting as per cancer type neoplastic cells growth and immune infiltration

https://doi.org/10.1515/oncologie-2022-1002
Received December 7, 2022; accepted February 24, 2023;
published online March 23, 2023

Abstract

Objectives: The *EVI2B* (Ecotropic Viral Integration Site 2B) gene encodes a transmembrane glycoprotein pivotal in immunocytes maturation. Recent evidence implicated EV12B's expression with human colon cancer progression. However, EVI2B's downstream pathways affecting tumor growth and tumor-infiltrating cells remain unclear.
Methods: We first studied the diagnostic and prognostic value of EVI2B in pan-cancers by utilizing a series of in silico tools and clinical samples. Then we identified the modulated transcriptional expression and DNA methylation in high *EVI2B*'s expression groups of the same three cancers. We verified via RT-PCR the effect of stable EVI2B knock-down on the expression of JAK/STAT-related genes in two immune cell lines and the acceleration of proliferation in four cancer cell lines. Finally, the regulation of leukocyte infiltration was studied using TIMER.
Results: In SKCM and LUAD a heightened *EVI2B*'s expression promoted a better prognosis. Conversely, in LGG EVI2B's upregulation concurred with a worse prognosis. EVI2B silencing enhanced the proliferation of the tumor cell lines. The hypermethylated genome strengthened EVI2B's Janus-like effect in high EVI2B expressing SKCM and LUAD tumors. While the total DNA methylation was lower in high *EVI2B* expressing LGG. Further analysis revealed that multiple EVI2B-involved down-stream JAK-STAT genes also exhibited the Janus-like feature in SKCM, LUAD and LGG progression. Correspondingly, anti-tumor leukocytes infiltrated *EVI2B* high expressing SKCM and LUAD while more pro-tumor ones penetrated into EVI2B heightened LGG.
Conclusions: *EVI2B* acts as a Janus-faced oncogene/anti-oncogene by differently affecting neoplastic cell proliferation rates and tumor-promoting or tumor-hindering immunocytes' infiltration.

Keywords: DNA methylation; EVI2B; JAK-STAT; oncological immunology; prognostic marker; tumor growth.

Introduction

Skin cutaneous melanoma (SKCM), lung adenocarcinoma (LUAD) and low-grade glioma (LGG) are ranked among the top causes of cancer death worldwide. Statistics indicate that lung cancer accounted for 11.6% (>2 million cases) of all tumor cases and 18.4% (>1.7 million cases) of total cancer deaths worldwide in 2018, wherein LUAD, a primary subtype of lung cancer, was most common in females and non-smoking males [1, 2]. Besides, gliomas accounted for approximately 80% of all new primary malignant brain and central nervous system tumors [3]. Typically, gliomas are

Fangyingnan Zhang and Xinning Wang contributed equally to this work.

***Corresponding authors: Chao Zhang**, School of Biomedical Engineering, Sun Yat-sen University, Guangzhou 510000, Guangdong, People's Republic of China, E-mail: zhchao9@mail.sysu.edu.cn; and **Zhibin Li**, Department of Burn and Plastic Surgery, Shenzhen Institute of Translational Medicine, Shenzhen 518035, Guangdong, People's Republic of China, E-mail: lzbszu@163.com
Fangyingnan Zhang, School of Biomedical Engineering, Sun Yat-sen University, Guangzhou, Guangdong, People's Republic of China; and Department of Burn and Plastic Surgery, Shenzhen Institute of Translational Medicine, Shenzhen, Guangdong, People's Republic of China
Xinning Wang, School of Life Sciences, Sun Yat-sen University, Guangzhou, Guangdong, People's Republic of China
Xiaoqi Zhang, The Center for Drug Research and Development, Guangdong Pharmaceutical University, Guangzhou, Guangdong, People's Republic of China
Saquib Waheed and Rong Zhong, Department of Burn and Plastic Surgery, Shenzhen Institute of Translational Medicine, Shenzhen, Guangdong, People's Republic of China
Ubaldo Armato, Jun Wu, Anna Chiarini and Ilaria Dal Prà, Department of Burn and Plastic Surgery, Shenzhen Institute of Translational Medicine, Shenzhen, Guangdong, People's Republic of China; and Section of Human Histology & Embryology, Department of Surgery, Dentistry, Pediatrics & Obstetrics, University of Verona, Verona, Venetia, Italy

classified into four grades, with Grade I and Grade II representing low-grade gliomas (LGGs) [4]. The glioblastoma (Grade IV) exhibits an overall ~15 months survival time while LGG has a much longer-lasting clinical course while proceeding to higher grades. It makes LGG a more suitable stage for intervention [5]. Additionally, SKCM causes 55,500 fatalities annually, accounting for 1.7% of the newly diagnosed cases of all cancer types. Compared with gliomas, SKCM's prevalence rate is lower, but since 1970 it has been rapidly increasing. Nowadays, SKCM causes the highest number of metastatic skin cancer-related deaths. Hence, developing more sensitive and precise biomarkers to diagnose and treat these malignancies is critical.

By negatively regulating the RAS pathway, the *NF1* gene is the major suppressor of neurofibromatosis [6]. *NF1* mutant is present in over 15% of all SKCM cases [7]. Various lines of evidence have shown that *EVI2B*'s (Ecotropic Viral Integration Site 2B) (aka CD361) expression is closely related to *NF1*'s transcription [8]. *EVI2B* is a protein encoding gene placed within the 27b intron of the *NF1* gene, having the complementary sequence of the latter. Using an *EVI2B*$^{-/-}$ (KO) murine model, Zjablovskaja et al. showed that *EVI2B* is a frequent integration site of murine leukemia retroviruses, being also a target of the transcription factor CCAAT/enhancer binding protein-(C/EBP-α), and promoting the function of granulocytic and hematopoietic progenitor cells [9]. EVI2B also participates in differentiating melanocytes and keratinocytes [8]. Moreover, EVI2B is a potential prognostic biomarker in colorectal cancer, osteosarcoma [10, 11] and metastatic melanoma [12]. Its product, EVI2B, is a transmembrane glycoprotein that regulates the tumor immune system.

Recent experimental evidence proved that tumor-infiltrating lymphocytes (TILs) profoundly influence neoplastic progression. Cancer cells function as antigens in human tissues, and a group of TILs can directly kill cancer cells thereby suppressing or slowing tumorigenesis. Conversely, other types of TIL function as tumor promoters [13, 14]. Besides the specific TIL types, the cancer's histopathological type and stage affect the patients' prognosis [15]. It was reported that via an IFN-γ-activated CD8$^+$ T cells infiltration high *EVI2B*'s expression acted as a favorable prognostic or antitumor factor in metastatic melanomas [12]. However, it was unclear whether EVI2B directly affects the proliferation of cancer cells and promotes an antitumor immunocytes infiltration in all types of cancers.

In this study, we first analyzed the public dataset regarding the patients of 33 types of common cancers from The Cancer Genome Atlas (TCGA). Next we checked EVI2B's cancer diagnostic features in SKCM using clinical tumor specimens. Subsequently, we assessed the relationship between *EVI2B*'s high or low expression levels and pan-cancer patients' survival via Gene Expression Profiling Interactive Analysis (GEPIA). Moreover, by stably silencing *EVI2B* in two immune cell lines (i.e. U937 and JURKAT) we explored the effects of *EVI2B*'s transcription on tumor immunity-related pathways in the absence of TILs. Besides, using the CCK-8 and colony formation assays we assessed whether EVI2B directly regulated the proliferation rates of four cancer cell lines (i.e. A375, A549, HepG2, and U87). Our results showed that an increased *EVI2B*'s expression correlated with a better prognosis in SKCM and LUAD but concurred with shorter survival in LGG patients. We also found the six key leukocyte groups in the tumors' microenvironments, i.e., CD4$^+$ T cells, CD8$^+$ T cells, B cells, macrophages, dendritic cells (DC), and neutrophils, were all up regulated in the patients with an *EVI2B*'s increased expression. On the other hand, the JAK-STAT and PI3K-Akt-NF-κB signaling axis was up-regulated in all three types of cancers investigated. However, STAT4 was upregulated in SKCM and LUAD, while STAT6 was upregulated in LGG. Therefore, STAT6 specifically drove the downstream infiltration of tumor-promoting Th2 cells in LGG, while STAT4 activated the anti-tumor Th1 cells in SKCM and LUAD. These results proved why EVI2B exerts distinct effects on the survival of SKCM, LUAD, and LGG patients.

Methods

Clinical specimens and immunochemistry

The First Affiliated Hospital of Shenzhen University provided us with all the melanoma samples. The EVI2B glycoprotein antibody (3263S) used was bought from Cell Signaling Technology, Inc. Immunochemistry experiments were conducted as described previously [16]. Briefly, the paraffin-embedded tissue was cut into 4-μm-thick sections. The antigen retrieval was done by boiling the samples for 10 min in a 0.01 M citric acid solution (pH=6) then cooling them down. Next, the slides were blocked with 3% H_2O_2 solution and 5% goat serum at 37 °C for 1 h. The EVI2B antibody (CST 3263S) was diluted by 1:1,000, and the slides were incubated at 4 °C overnight. Sections were next incubated with a secondary antibody, and diaminobenzidine tetrachloride (DAB) served to develop the peroxidase reaction. The HMB-45 (38815S) and S-100 (90393) antibodies were also purchased from Cell Signaling Technology, Inc. (Danvers, Massachusetts, USA). The Melan-A (M02033) antibody was purchased from Boster Biological Technology Co., Ltd (Wuhan, Hubei, CHN).

Establishment of stable EVI2B-silenced cell lines

We used the GL427 lentivirus expression vector (OBiO Technology Corp., Ltd.; Shanghai, CHN) to deliver the *EVI2B* shRNA into U937, Jurkat, A549, A375, HepG2, and U87cells. U937 is a macrophage-like

lymphoma cell line. Jurkat is a T lymphocyte leukemia cell line. All the cells were purchased from Procell Life Science & Technology Co., Ltd (Wuhan, Hubei, CHN). A scrambled siRNA sequence served as the negative control. The shRNAs sequences used were: *EVI2B* Si-1: CACAGCCTACCTTATTCACAT; *EVI2B* Si-2: CCAATCTGACAAACCCACAAT; *EVI2B* Si-3: CCAACTCTGATCAAGATCTTA; NC: CCTAAGGTTAAGTCGCCCTCG. The A549, A375, U87 and HepG2 cells were cultured in DMEM (Gibco, 11965092) with 10% FBS (Gibco, 10,099) and 1% Pen-Strep solution (Gibco, 15140148) added. The U937 and Jurkat cells were cultured in RPMI 1640 medium (Gibco, 61870036) with 10% FBS (Gibco, 10099) and 1% Pen-Strep solution (Gibco, 15140148). All the cell culture medium was produced by Thermo Fisher Scientific Co., Ltd (Waltham, Massachusetts, USA). Cultures were run at 37 °C in air 95%/CO_2 5% v/v.

Cell proliferation assay

EVI2B-silenced A549, A375, HepG2 and U87cells were seeded at 200 cells/well in 96-well plates and cultured for 48 h at 37 °C in the air with 5% v/v CO_2. Non-silenced corresponding control cells were seeded in parallel and treated similarly. The cell growth rate was evaluated using the Cell Counting Kit-8 (#HY-K0301, MCE, New Jersey, USA). The cells' absorbance represented the relative cell numbers.

A colony formation assay assessed the proliferation rate changes in the *EVI2B*-silenced cell lines. One hundred A549 cells were seeded onto 100 mm dishes and cultured for one week to obtain the colonies. The area of the colonies was evaluated using Image J software.

RNA extraction and real-time (RT-PCR)

The *EVI2B*-silenced U937 and Jurkat cells were collected 72 h after lentivirus transfection and next lysed with TRIZOL reagent (#15596018, Invitrogen, Waltham, Massachusetts, USA). Chloroform was added to extract the RNA and isopropanol was used to collect the RNA precipitates. After being washed with ice-cold 70% ethanol, the RNA pellets were dissolved in DEPC-treated water. The cDNA was synthesized using the Fist strand cDNA synthesis kit (Thermo, #K16225). The RT-PCR was conducted according to the manufacturer's instructions (#B21202, Bimake, Shanghai, CHN). The PCR primers were designed by using the PrimerBank database (pga.mgh.harvard.edu) and are shown in Table S1.

Western immunoblotting

The cell samples were lysed through sonication in RIPA buffer (#20101ES, Yeason, Nanjing, Jiangsu, CHN) with added protease and phosphatase inhibitors (Roche, Monza, Italy). The BCA assay kit (Thermo Fisher, #23227) assessed the protein concentration and assured that equal protein amounts were loaded to all lanes. After SDS-PAGE electrophoresis, proteins were blotted onto PVDF membranes. 5% skimmed milk was applied to block the non-specific binding antigen. The primary antibodies were incubated overnight at 4 °C. TBST buffer (Thermo Fisher, #37543) was used to wash the membrane three times. The second antibodies were incubated at room temperature for 1 h. After three washes, the membranes were incubated with HRP substrate (#WBKLS0100, Millipore, KGaA, Darmstadt, Germany) to detect the bands. The protein band density was measured with ImageJ software.

Genetic and prognostic analysis using GEPIA

GEPIA was used to assess the expression levels of *EVI2B* and differential survival rates between high and low *EVI2B*'s expression groups in all 33 cancer types from TCGA and GTEx (Genotype-Tissue Expression project). GEPIA is available at http://gepia.cancer-pku.cn/ [17]. The cancer types were labeled according to TCGA (The Cancer Genome Atlas) (ACC: Adrenocortical carcinoma, BLCA: Bladder Urothelial Carcinoma, BRCA: Breast invasive carcinoma, CESC: Cervical squamous cell carcinoma and endocervical adenocarcinoma, CHOL: Cholangio carcinoma, COAD: Colon adenocarcinoma, DLBC: Lymphoid Neoplasm Diffuse Large B-cell Lymphoma, ESCA E: sophageal carcinoma, GBM: Glioblastoma multiforme, HNSC: Head and Neck squamous cell carcinoma, KICH: Kidney Chromophobe, KIRC: Kidney renal clear cell carcinoma, KIRP: Kidney renal papillary cell carcinoma, LAML: Acute Myeloid Leukemia, LIHC: Liver hepatocellular carcinoma, LUSC: Lung squamous cell carcinoma, MESO: Mesothelioma, OV: Ovarian serous cystadenocarcinoma, PAAD: Pancreatic adenocarcinoma, PCPG: Pheochromocytoma and Paraganglioma, PRAD: Prostate adenocarcinoma, READ: Rectum adenocarcinoma, SARC: Sarcoma, STAD: Stomach adenocarcinoma, TGCT: Testicular Germ Cell Tumors, THCA: Thyroid carcinoma, THYM: Thymoma, UCEC: Uterine Corpus Endometrial Carcinoma, UCS: Uterine Carcinosarcoma, UVM: Uveal Melanoma).

Differentially expressed genes (DEGs) analysis via c-Bioportal

The c-Bio Cancer Genomics Portal (http://cbioportal.org) was used to analyze the differentially expressed genes (DEGs) [18]. The 469 SKCM, 619 LGG and 586 LUAD samples of the TCGA and Firehouse Legacy Project were divided into two groups according to *EVI2B*'s expression levels, respectively. The *EVI2B* high expression individuals were determined by standard score and the threshold was Z-score >1.

The DNA methylation data was obtained based on human methylation HM450 chip from the c-Bioportal database. A t-test determined the significance of methylation changes.

DEG genes analysis via DAVID and KEGG

The Database for Annotation, Visualization, and Integration Discovery (DAVID) interprets the functions of an extensive list of genes. Modules of Gene Ontology (GO) annotation and KEGG (Kyoto Encyclopedia of Genes and Genomes) pathway analysis were integrated into DAVID. We used DAVID to perform the DEGs clustering. DAVID is available at http://david.niaid.nih.gov [19].

Immunocytes infiltration analysis via TIMER (tumor immune estimation resource)

The TIMER (http://cistrome.shinyapps.io/timer) software served to quantify the immunocytes infiltration [20]. The analysis was based on the transcriptomic data of TCGA. Each patient's EVI2B expression level was exported along with certain immunocyte infiltration levels or an immunocyte marker gene level. The correlation between *EVI2B* expression and immune infiltration was determined via further

statistical analysis. With multiple immune infiltration algorithms provided, we used TIMER2 to validate the finding.

Data availability and statistical analysis

All the source data of omics has been uploaded to Github and can be downloaded at https://github.com/zfyn/EVI2B-data/tree/main.

The divergent levels of *EVI2B* expression were assessed based on the Standard Score, a statistical parameter evaluating the degree of deviation. The individuals with Z-score >1 were defined as the high *EVI2B* expression group. The identity of the DEGs was proved via Student's *t*-test with a p-value <0.05. The differentially methylated genes were identified via Student's *t*-test with a p-value <0.05. The R-value of the Spearman test and p-value of the Student's *t*-test was used to assess the correlation between *EVI2B* expression and immune cell marker genes levels. r>0 represented the positive correlation. The confidence of the clustering annotation was evaluated via false discovering rate (FDR) for the DAVID-GO enrichment of DEGs.

Results

EVI2B's expression affected the survival prognosis of SKCM, LUAD, and LGG cases

Using the GEPIA database we investigated *EVI2B*'s expression levels in 33 types of tumors compared to their normal tissue counterparts. Figure 1A shows that EVI2B was upregulated in 11 diverse types of cancers, including esophageal carcinoma (ESCA), glioblastoma multiforme (GBM), kidney renal clear cell carcinoma (KIRC), kidney renal papillary cell carcinoma (KIRP), acute myeloid leukemia (LAML), LGG, ovarian serous cystadenocarcinoma (OV), pancreatic adenocarcinoma (PAAD), SKCM, stomach adenocarcinoma (STAD), and testicular germ cell tumors (TGCT). In contrast, EVI2B was significantly downregulated in diffuse large B-cell lymphoma (DLBC), lung squamous cell carcinoma (LUSC), and thymoma (THYM) (Figure 1B). Concerning the tumorigenesis process, *EVI2B* expression fluctuated during distinct stages of SKCM progression (Figure 1C).

To assess the reliability of the high-throughput data, we examined immunohistochemistry EVI2B protein's levels in clinical tumor specimens. For example, Figure 1D shows that melanoma tumor cells could be identified via the biomarkers HMB-45, Melan-A, and S-100. The EVI2B glycoprotein was upregulated in the melanoma cells as compared to the adjacent normal tissue, consistent with the GEPIA data.

To evaluate whether EVI2B was associated with the potential prognosis of various tumors, we used GEPIA to analyze the survival data from 33 distinct types of cancer (Figure 2A). Interestingly, *EVI2B*'s expression significantly affected the prognosis in LUAD, LGG, and SKCM. The *EVI2B* high-expression patients had a shorter-lasting survival in LGG (HR [high]=2.3, P[HR]=$2.3e^{-5}$) but a longer-lasting one in LUAD (HR [high]=0.65, P[HR]=0.0058) and SKCM (HR [high] =0.49, P[HR]=$2.7e^{-7}$) (Figure 2B). We could confirm EVI2B's prognostic value in LGG, LUAD, and SKCM cases by comparing the survival curves with the high or low *EVI2B*'s expression levels and grouping them according to gradient inclusion criteria (Figures S1 and S2).

EVI2B's expression levels correlated with JAK-STAT and PI3K-Akt pathways

To elucidate the underlying signaling pathways regulating the prognosis in *EVI2B*-high-expressing patients, we performed a cluster analysis of the DEGs pertaining to *EVI2B* high- and low-expressing groups. The gene expression data were extracted from the TCGA database and the Firehouse Legacy datasets. Via c-Bioportal the samples were divided into high *EVI2B* expression and low *EVI2B* expression groups, respectively. Next, the genes with p-values <0.05 were listed and selected as the DEGs of LUAD, SKCM, and LGG. To conduct the KEGG pathway clustering analysis, we chose the up-regulated DEGs with the lowest 1,000 p-values. As Figure 3A–C show, the JAK-STAT signaling pathway, NF-κB signaling pathway, PD-L1 (programmed cell death ligand 1) expression, PD-1 (programmed cell death protein 1) checkpoint pathway, and PI3K-Akt signaling pathway were clustered in all three types of cancers. We further analyzed DEGs based on their expression fold-changes and found that the target genes of the JAK-STAT signaling pathway (i.e. JAK3, PIK3CG, CSF1R, and PIK3R5 of the PI3K-Akt pathway, and TLR4 and VCAM1 of the NF-κB pathway) were up-regulated more than two-fold in all three types of cancer (Figure 3D).

Additionally, we investigated the downregulated DEGs. In contrast to the consistency of the up-regulated DEGs clustering, the down-regulated DEGs of LGG significantly diverged from those of LUAD and SKCM. As shown in Figure 3E–G, mitochondrial and RNA metabolism-related genes were downregulated in LUAD and SKCM. On the other hand, most of the pathways clustered in LGG were associated with the nervous system. These results clarify why EVI2B regulates distinct signaling pathways linked to LGG infiltrating immunocytes and the patient's prognosis. Additionally, the analysis of JAK-STAT pathway genes in relation to survival showed divergent results. The JAK3, STAT4, and STAT5A genes differently affected the patients' survival in LGG, LUAD, and SKCM, respectively (Figure 4).

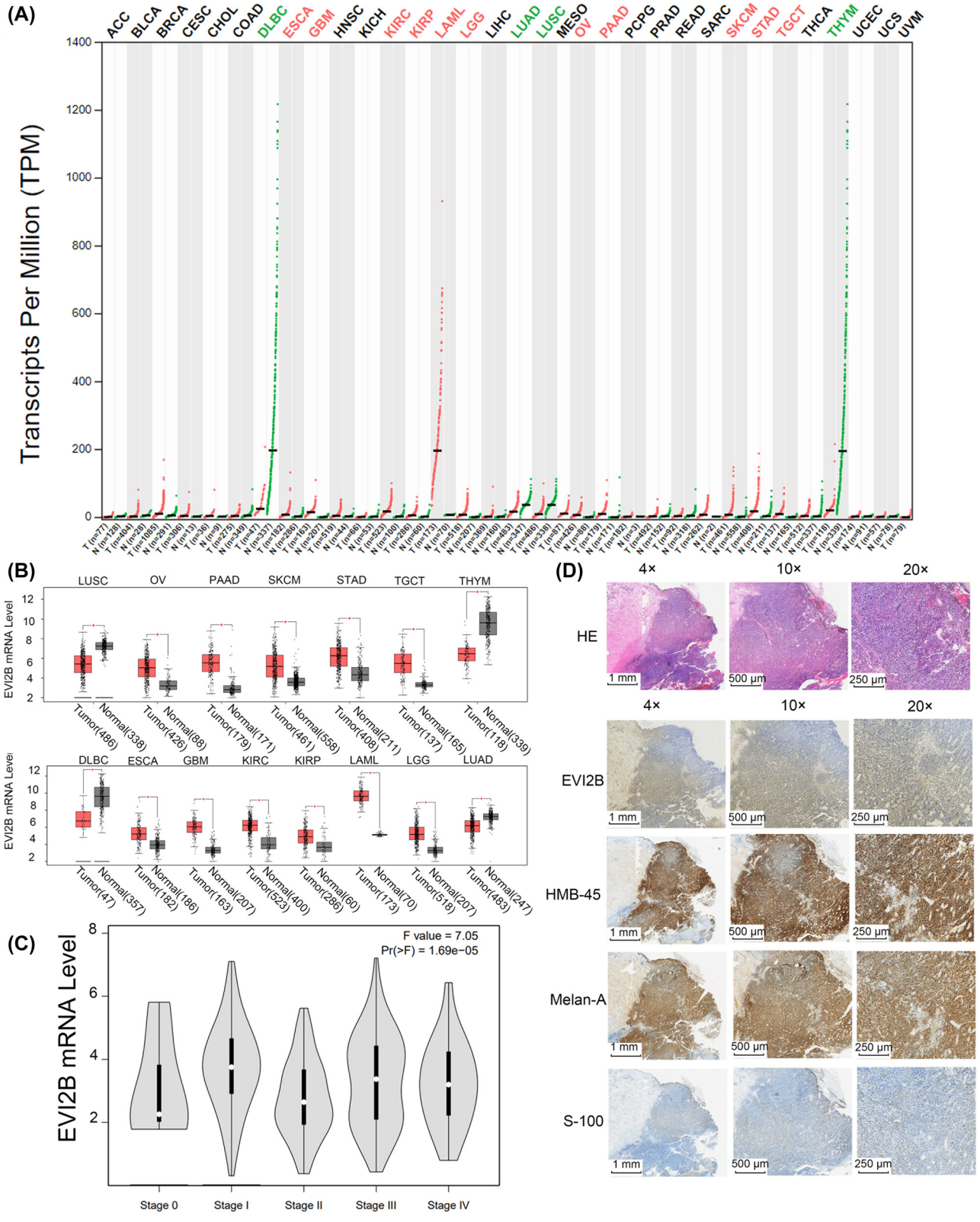

Figure 1: *EVI2B*'s expression levels of in a variety of human cancers. (A) *EVI2B*'s expression in 33 cancer types vs. their normal tissue counterparts. The names of tumors with up-regulated EVI2B are in red, while those of tumors with downregulated EVI2B are in green. (B) *EVI2B* expression levels differed in 15 types of cancers, including LUAD, LGG, and SKCM. *EVI2B* expression levels were significantly higher in LGG and SKCM than in the counterpart normal tissues. (C) *EVI2B* expression levels in various stages of SKCM. (D) H&E staining and immunohistochemistry staining of the melanoma markers HMB-45, Melan-A, and S-100 defines the tumor area. The *EVI2B* expression merged with the other markers indicated its diagnostic value.

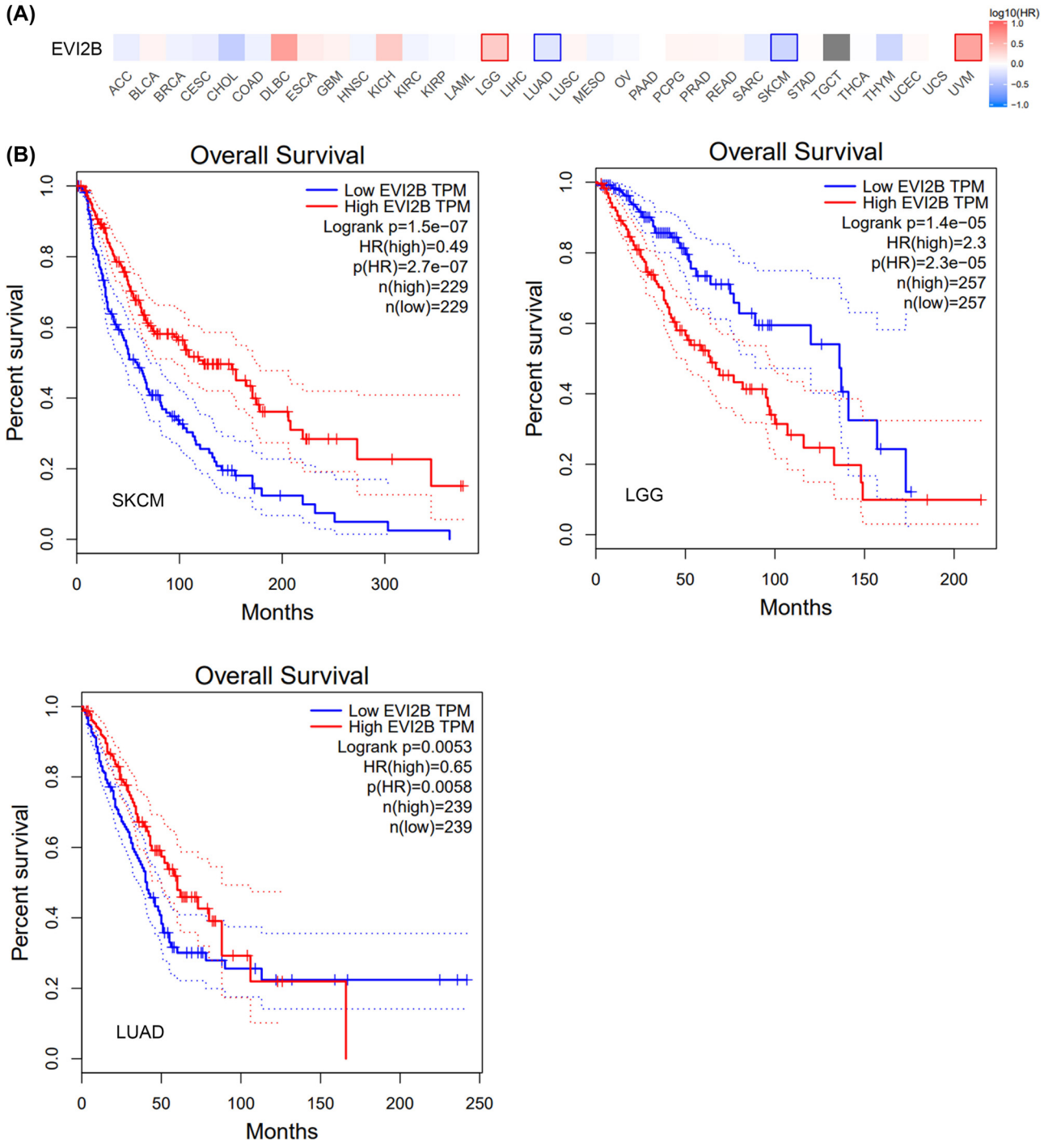

Figure 2: Patients' survival curves as related to high (red boxes) and low (blue boxes) *EVI2B* expression levels in 33 cancer types as analyzed via GEPIA. The cancer types with a significantly negative correlation with the increased *EVI2B*'s expression are labeled as red boxes with frames. Conversely, blue boxes with frames denote the cancer types that positively correlate with the increased *EVI2B* expression. (B) The overall survival curves of different tumors in relation to the *EVI2B*'s high and low expression levels.

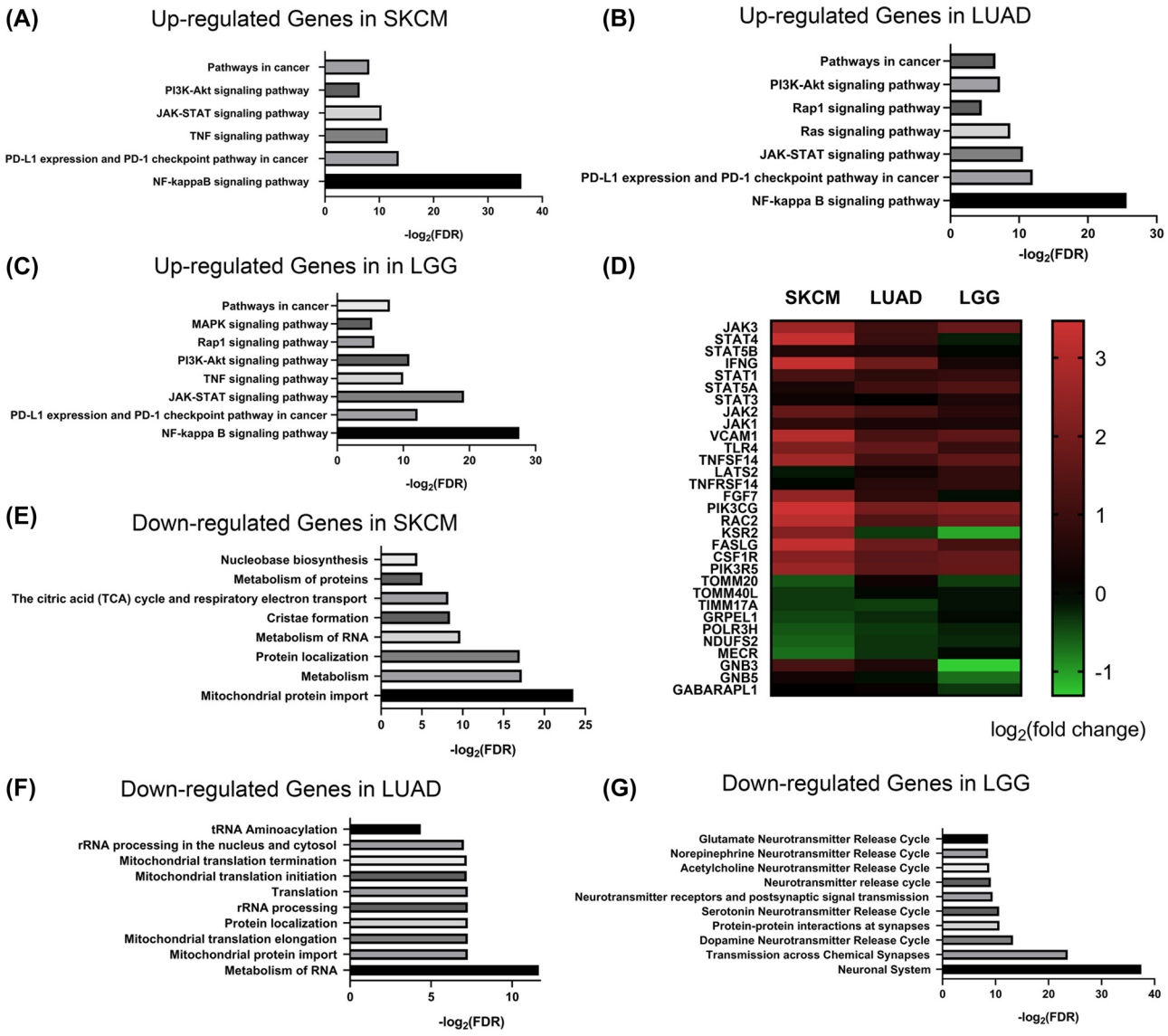

Figure 3: Clustering analysis of the differentially expressed genes (DEGs) in *EVI2B* highly expressing tumor patients. (A–C) The DAVID-GO enrichment of up-regulated DEGs. The confidence of the clustering annotation was evaluated via false discovering rate (FDR)]. A larger -LOG2(FDR) value represented a more confident clustering. (D) Heat map of DEGs in high *EVI2B* expression samples of SKCM, LUAD and LGG. The grouping standard for high *EVI2B* expression or low *EVI2B* expression was based on a standard score. Individuals whose *EVI2B* expression was upregulated and met the threshold Z>1 were grouped as high *EVI2B* expression. The rest were identified as low *EVI2B* expression. (E–G) The DAVID-GO enrichment of down-regulated DEGs.

EVI2B's expression affects total genomic methylation/demethylation including genes of JAK-STAT and PI3K-Akt signaling pathways

A shift in DNA methylation pattern often goes along with tumorigenesis. Hypermethylation is an important mechanism involved in the inhibition of gene transcription. To figure out whether there might be any correlation between EVI2B and DNA methylation, we obtained the DNA methylation chip data from the TCGA database and Firehouse Legacy data set and further examined the overall methylation profile of LUAD, LGG and SKCM samples between the *EVI2B* high- and low-expression groups. The divergence of methylation level was determined by *t*-test. Genes whose methylation level changed with a p-value <0.05 were identified as hypermethylated and demethylated. As to SKCM, the high *EVI2B* expressing group had 5,022 genes with increased methylation, while in the low *EVI2B* expressing group 4,315 genes were hypermethylated. As to LUAD, the high *EVI2B* expressing group had 3,614

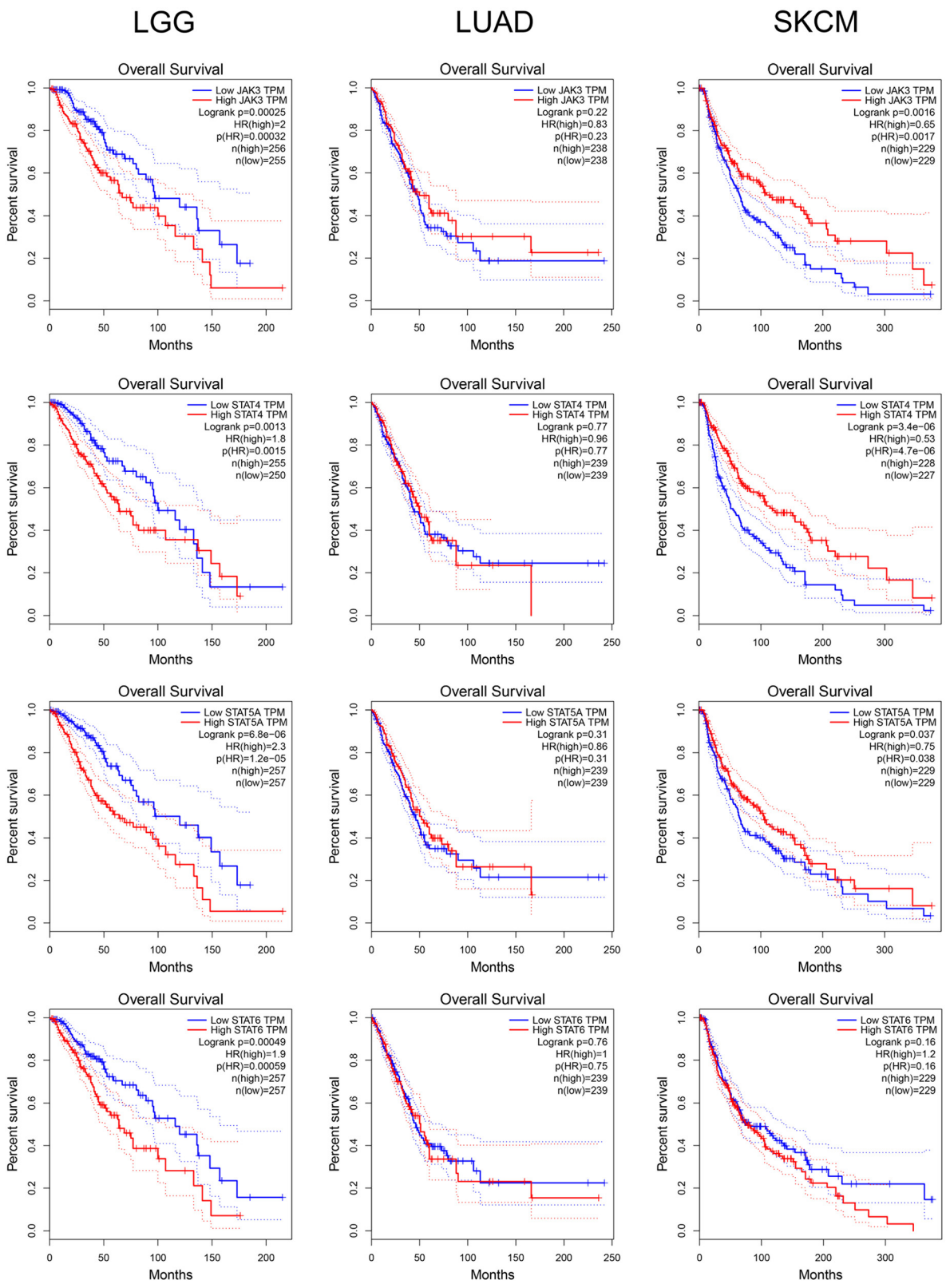

Figure 4: Survival analysis of EVI2B down-stream genes. The survival curves of EVI2B down-stream JAK-STAT genes were analyzed. Up-regulation of the JAK-STAT genes behaved differently according to the prognosis in SKCM and LUAD concerning to LGG.

genes with higher methylation levels, while the low *EVI2B* expressing group had 2,396 hypermethylated genes. As to LGG, the overall genomic methylation levels were lower; the high *EVI2B* expressing group had 1,636 hypermethylated genes, while the *EVI2B* low expression group had 5,083 genes with increased methylation levels (Figure 5A). Interestingly, as had happened for prognosis, down-regulated DEGs, and immunocytes infiltration (see below), *EVI2B* expression similarly affected DNA methylation in LUAD and SKCM but not in LGG. The high *EVI2B* expressing group showed more intense methylation in LUAD and SKCM, but a less intense one in LGG.

Moreover, Figure 5B–D show that the genes of the JAK-STAT and PI3K-Akt pathways were demethylated along with *EVI2B*'s high expression. Typically, JAK3, STAT3, PIK3GC, PIK3R5, and RAC2 were demethylated in all three types of cancer. By comparison, JAK1, VCAM1, and KSR2 genes were only demethylated in SKCM and LUAD. Moreover, the protein-protein interaction analysis of the upregulated and demethylated genes revealed that the JAK-STAT genes were closely related to the PI3K-Akt genes (Figure 5E). Therefore, by demethylating essential genes, EVI2B can activate the JAK-STAT and PI3K-Akt pathways in SKCM, LUAD, and LGG.

EVI2B's expression levels affected the growth of four diverse cancer cell lines

To evaluate the impact of EVI2B on tumor cells, we examined the cell viability while *EVI2B* was silenced in four cancer cell lines (A375, A549, U87 and HepG2). RT-PCR quantified the knock-down efficiency of shRNA with two pairs of *EVI2B* primers, which guaranteed accuracy (Figure 6A). The CCK-8 assay indicated that when *EVI2B* was silenced, all four cancer cell lines exhibited accelerated proliferation rates, which suggested *EVI2B* functioned as an anti-oncogene (Figure 6B). The idea EVI2B can regulate cancer cell division was re-validated via colony formation assay. Consistently, the EVI2B knock down cells showed a higher colony number and a significantly larger colony area (Figure 6C).

EVI2B's expression levels correlated with tumor-infiltrating immunocytes in LUAD, LGG, and SKCM

Immunocyte infiltration significantly alters cancer progression via various mechanisms, including assisting neoplastic cells in evading the immune system or promoting resistance to multiple drugs. We analyzed the correlation between *EVI2B*'s expression levels and cancer-infiltrating immunocytes using TIMER in 33 types of neoplasia. As Figure 7 shows, statistical analysis revealed that *EVI2B*'s expression correlated with immunocytes infiltration of SKCM, LUAD, and LGG-a finding multiple immunocytes infiltration algorithms further confirmed (Figure S3). *EVI2B*'s expression significantly affected the prognosis of the three cancer types as it positively correlated with the distinct kinds of immunocytes infiltrating SKCM, LUAD, and LGG.

To gain the immunocytes infiltration details, we analyzed the correlation between *EVI2B*'s expression, and the markers sets of the immunocytes penetrating into LUAD, LGG, and SKCM, that is $CD8^+$ T cells, T cells (generic), B cells, monocytes, tumor-associated macrophages (TAMs), M1 and M2 polarized macrophages, neutrophils, NK cells, and DCs (Table 1). Moreover, we analyzed the functional differences among T cell sets, such as Th1 cells, Th2 cells, T follicular helper (Tfh) cells, Th17 cells, regulatory T cells (Tregs), and exhausted T cells (Figure 8).

We found that EVI2B promoted the $CD8^+$ T cells, $CD4^+$ T cells, and macrophages infiltration in LUAD, LGG, and SKCM. The R-values of $CD8^+$ T cells in LUAD (R=0.538) and SKCM (R=0.635) were higher than in LGG (R=0.317). The R-values of $CD4^+$ T cells and macrophages in LUAD (R=0.554) and SKCM (R=0.539) were lower than in LGG (R=0.836) (Figure 7). In fact, in LGG the T cell markers CD8A, CD8B, STAT4, STAT5B, CCR8, and FOXP3 behaved differently. As is clear from the graph, the immune markers of B cells and exhausted T cells had a robust positive relationship with *EVI2B* expression in LUAD and SKCM but showed a weaker correlation in LGG. The Spearman's correlation coefficients for CD19, CD79A, PD-1, and CTLA-4 were all positive and prominent in LUAD and SKCM. Conversely, the correlation coefficients for LGG were much lower than those for LUAD and SKCM (Table 1). *EVI2B* expression concurred with biomarkers (STAT5 and STAT6) for Th2 cells, a kind of $CD4^+$ T cells, in LGG (R_{STAT5A}=0.745, R_{STAT6}=0.576). In contrast, STAT5 and STAT6 showed a much weaker relation to EVI2B in SKCM (R_{STAT5A}=0.264, R_{STAT6}=0.105) and STAT6 also showed no correlation to EVI2B in LUAD (R_{STAT5A}=0.734, R_{STAT6}=0.184). Additionally, Th1 cell markers also showed this contrary trend (SKCM R_{STAT4}=0.806, LUAD R_{STAT4}=0.579, LGG R_{STAT4}=−0.121; SKCM R_{TBX21}=0.805, LUAD R_{TBX21}=0.647, LGG R_{TBX21}=−0.2) (Table 1).

Moreover, the immunological markers of dendritic cells, monocytes, and M2 macrophages showed a strong positive correlation with *EVI2B* expression in all three types of cancers examined. Table 1 also indicates that HLA-DPB1, HLA-DQB1, VSIG4, CD86, and CSFR1 were upregulated along with EVI2B ($p<0.0001$; $R\approx1$), respectively,

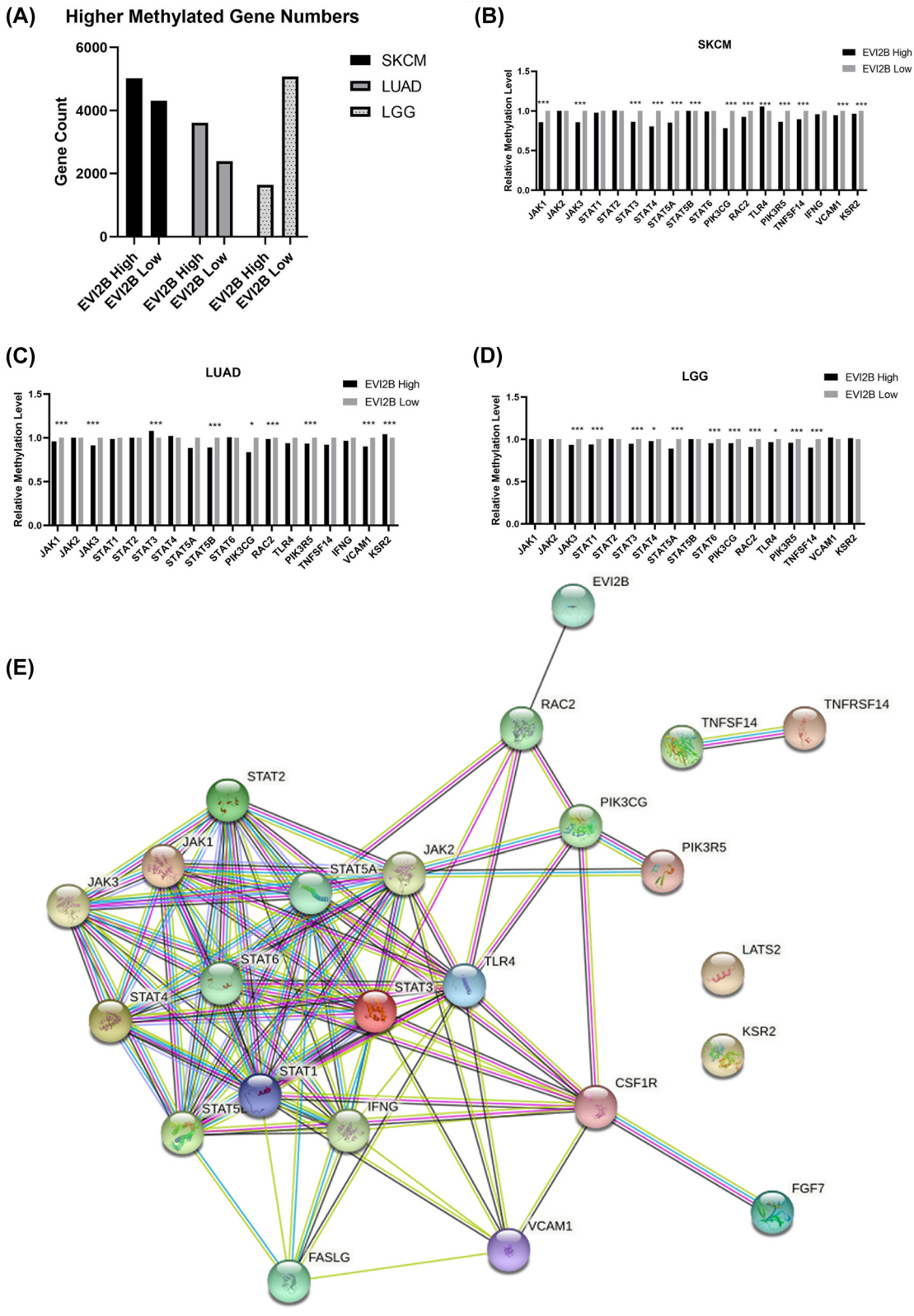

Figure 5: *EVI2B*'s high and low expression levels in SKCM and LUAD affected the methylation of the whole genome and of genes related to the JAK/STAT and PI3K/Akt pathways differently from what they did in LGG. (A) The total numbers of methylated genes according to the high or low *EVI2B* gene expression in SKCM, LUAD an LGG. The grouping standard for high and low *EVI2B* expression was stated in Figure 3A legend. (B–D) The relative changes in specific genes methylation levels of SKCM, LUAD, and LGG in the high-*EVI2B* expressing vs. the low-*EVI2B* expressing tumors. The partly similar SKCM's and LUAD's patterns differ from LGG's. The differentially methylated genes were identified via Student's *t*-test. Genes with p-value <0.05 were considered as hypermethylated or demethylated. The methylation of multiple JAK-STAT genes was modulated by EVI2B. (E) The STRING pathway clustering of JAK/STAT proteins whose upregulation EVI2B mediates.

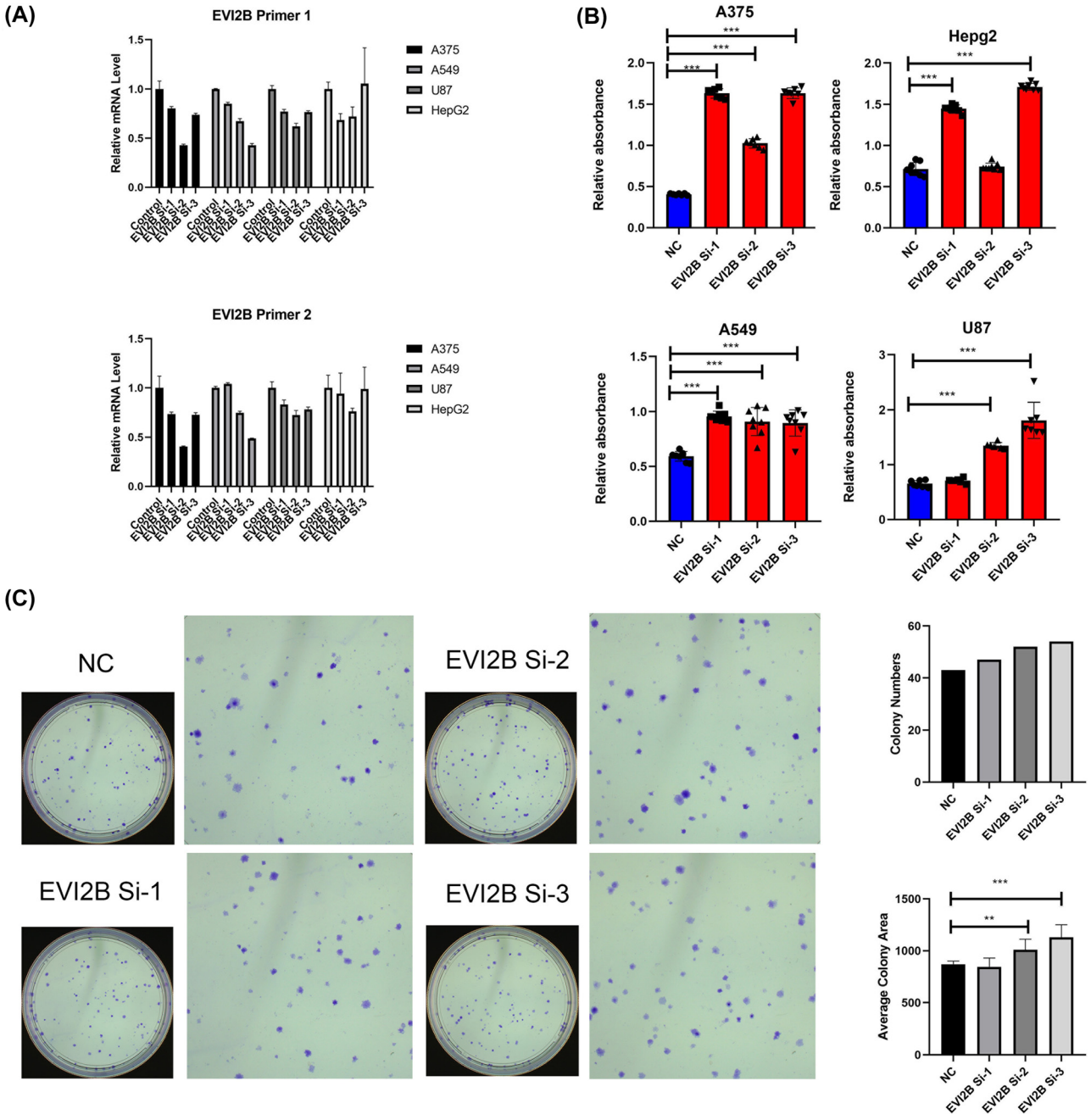

Figure 6: The results of EVI2B knock-down assay in A375 (melanoma), HepG2 (hepatoma), A549 (lung adenocarcinoma), and U87 (glioma) cell lines show that it directly acts on the tumor cells as an antioncogene. (A) RT-PCR analysis of *EVI2B*'s transcription levels in the four silenced cell lines studied. (B) Colony formation assay for the A549 cell line. (C) The CCK-8 assay results show that silencing EVI2B stimulated the proliferation in all four cell lines investigated proving that when functioning EVI2B is by itself (i.e., in the absence of tumor-infiltrating immunocytes) an antioncogene that significantly slows the growth of these neoplastic cell lines.

suggesting diversity in the roles played by EVI2B in different tumor microenvironments.

To further verify the function of EVI2B-mediated regulation of signaling pathways, via lentivirus we constructed EVI2B knock-down cell lines. In keeping with our earlier analysis (Figure 6), the study focused on the macrophage and T cell lines. Once EVI2B protein's silencing was obtained (Figure 9A), STAT4, STAT6, and TNF-α were sharply down-regulated in U937 and Jurkat cells. Moreover, the mRNA results showed that IFN-γ was also significantly down-regulated in Jurkat cells (Figure 9B). In summary, the clinical sample RNA sequencing data (Figure 3) and the RT-PCR

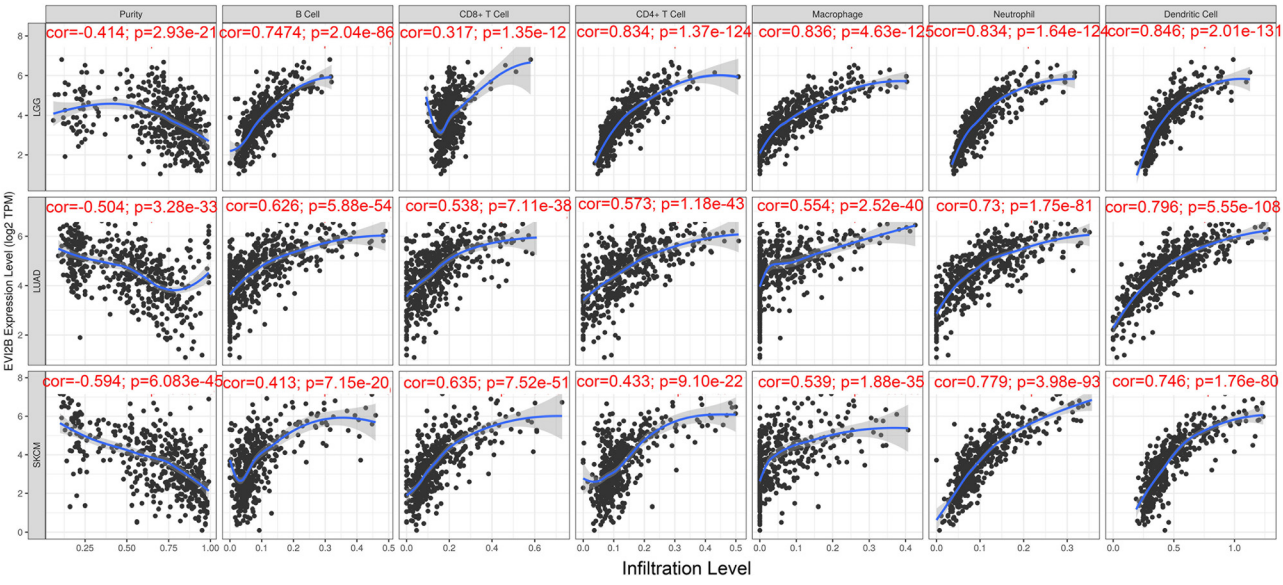

Figure 7: Correlation of *EVI2B*'s expression levels with the immunocytes' infiltrates in LGG, LUAD, SKCM. Scattered dots show the relationship between *EVI2B*'s expression levels and immunocytes infiltration. Each dot stands for a clinical sample. LGG (n=505); LUAD (n=482); SKCM (n=425). The blue continuous line means the average expression of EVI2B at each infiltration level. The R value of correlation analysis and p value for *t*-test are presented in red. The R>0 and p<0.05 represent the statistically significant positive relationship between EVI2B and immune infiltrates.

results (Figure 9B) showed that the JAK-STAT pathway is the down-stream target of EVI2B.

Discussion

The *EVI2B* gene encodes a plasma membrane glycoprotein involved in granulocyte development and hematopoietic progenitor cell activity [9]. However, little is still known about EVI2B's roles in other biological processes and cellular functions. Based on high throughput clinical data, we found that three types of cancers were significantly, though differently, influenced by EVI2B via the changes in the DNA methylation of genes involved in the JAK-STAT and PI3K-Akt signaling pathways. Yonekura and Ueda [12] reported that EVI2B promotes immune infiltration in melanoma. Our study integrating the overall cancer cell proliferation rates and signaling pathways with specific patterns of infiltrating immunocytes further revealed that, EVI2B modulates patients' prognosis in a pan-cancer view. Thus, a tissue-specific regulation mode of EVI2B affecting the activation of specific types of immunocytes resulted in quite divergent outcomes in LGG compared to LUAD and SKCM.

In this study, we first found that *EVI2B* expression globally reduced cell proliferation in various cancer cell lines, which suggested that *EVI2B* may function as an oncogene. However, this idea contradicted EVI2B's Janus-faced prognostic data. As to SKCM and LUAD, high *EVI2B* expression individuals showed better survival rates than the low *EVI2B* expression ones, which indicated that *EVI2B*'s role was antioncogenic. Conversely, as to LGG, the high *EVI2B* expression group showed a poorer survival, which connoted its role as an oncogene; this contrasted with the observation that after knocking down *EVI2B* expression the glioma cell line U87 showed an accelerated proliferation, which revealed that when expressed EVI2B played the role of an antioncogene in such cells.

The clustering analysis provided clues to explain this dilemma about the divergent tissue-specific effects of EVI2B on tumor progression. This analysis proved that multiple JAK-STAT pathway genes were associated with EVI2B, such as JAK3, STAT4, STAT5A and STAT6 (Figure 3D). Intriguingly, all these genes showed double-edged effects on cancer prognosis (Figure 4). Concretely, the high expression group of all the four genes showed poorer survival in LGG, at sharp variance with that in LUAD and SKCM. This Janus-faced role of EVI2B may be due to the double-edged feature of the JAK-STAT pathway. This view is strengthened by the fact that STAT4 and STAT6 were validated as down-stream effectors of EVI2B (Figure 9B).

The JAK-STAT pathway is an essential regulatory axis in tumor immunology. It is well known that the spatial heterogeneity of immunocytes infiltration in tumors has implications for cancer progression and outcome [21]. To date, mounting evidence proves that distinct types of immunocytes play a vital role in tumor infiltration. Besides,

Table 1: The correlation between immunocytes marker genes and EVI2B's expression levels in SKCM, LUAD and LGG, respectively. $CD8^+$ T cells, Th1 cells, Th2 cells, and others behaved in SKCM and LUAD differently from what they did in LGG.

Description	Gene markers	SKCM				LUAD				LGG			
		None		Purity		None		Purity		None		Purity	
		cor	p-Value	cor	p-Value	cor	p-Value	cor	p-Value	cor	p-Value	cor	p-Value
$CD8^+$ T cell	CD8A	0.788	***	0.681	***	0.639	***	0.541	***	0.258	***	0.143	**
	CD8B	0.764	***	0.636	***	0.53	***	0.444	***	0.257	***	0.163	***
T Cell (general)	CD3D	0.822	***	0.717	***	0.697	***	0.588	***	0.453	***	0.407	***
	CD3E	0.818	***	0.714	***	0.78	***	0.698	***	0.497	***	0.472	***
	CD2	0.851	***	0.771	***	0.792	***	0.716	***	0.502	***	0.488	***
B Cell	CD19	0.667	***	0.545	***	0.601	***	0.479	***	0.362	***	0.301	***
	CD79A	0.71	***	0.573	***	0.604	***	0.495	***	0.321	***	0.346	***
Monocyte	CD86	0.902	***	0.854	***	0.814	***	0.766	***	0.921	***	0.909	***
	CD115 (CSF1R)	0.841	***	0.779	***	0.768	***	0.717	***	0.846	***	0.812	***
TAM	CCL2	0.665	***	0.536	***	0.456	***	0.355	***	0.473	***	0.424	***
	CD68	0.559	***	0.425	***	0.685	***	0.632	***	0.826	***	0.805	***
	IL10	0.679	***	0.563	***	0.619	***	0.526	***	0.629	***	0.592	***
M1 macrophage	INOS (NOS2)	−0.036	0.437	−0.04	0.389	0.155	***	0.06	0.18	−0.132	**	−0.161	***
	IRF5	0.679	***	0.515	***	0.521	***	0.448	***	0.843	***	0.807	***
	COX2 (PTGS2)	0.133	***	0.069	0.138	−0.062	0.162	−0.067	0.136	0.17	***	0.108	*
M2 macrophage	CD163	0.745	***	0.661	***	0.688	***	0.631	***	0.484	***	0.493	***
	VSIG4	0.704	***	0.615	***	0.674	***	0.634	***	0.779	***	0.752	***
	MS4A4A	0.809	***	0.737	***	0.738	***	0.684	***	0.644	***	0.652	***
Neutrophils	CD66b (CEACAM8)	−0.018	0.701	0.022	0.64	0.329	***	0.35	***	0.046	0.3	0.045	0.33
	CD11b (ITGAM)	0.761	***	0.693	***	0.747	***	0.705	***	0.84	***	0.802	***
	CCR7	0.738	***	0.589	***	0.715	***	0.612	***	0.297	***	0.284	***
Natrual killer cell	KIR2DL1	0.382	***	0.243	***	0.168	***	0.103	**	0.002	0.963	0.04	0.38
	KIR2DL3	0.53	***	0.346	***	0.274	***	0.182	***	0.145	***	0.149	**
	KIR2DL4	0.622	***	0.465	***	0.254	***	0.166	***	0.437	***	0.455	***
	KIR3DL1	0.488	***	0.312	***	0.21	***	0.14	**	0.002	0.964	0.004	0.94
	KIR3DL2	0.599	***	0.44	***	0.326	***	0.239	***	0.166	***	0.172	***
	KIR3DL3	0.13	***	0.05	0.291	0.107	*	0.083	0.066	0.075	0.088	0.082	0.07
	KIR2DS4	0.415	***	0.287	***	0.274	***	0.207	***	0.175	***	0.161	***
Dendritic cell	HLA-DPB1	0.817	***	0.722	***	0.731	***	0.669	***	0.712	***	0.694	***
	HLA-DQB1	0.75	***	0.625	***	0.527	***	0.433	***	0.559	***	0.531	***
	HLA-DRA	0.861	***	0.792	***	0.734	***	0.671	***	0.77	***	0.756	***
	HLA-DPA1	0.809	***	0.726	***	0.744	***	0.694	***	0.723	***	0.709	***
	BDCA-1 (CD1C)	0.656	***	0.513	***	0.507	***	0.439	***	0.353	***	0.359	***
	BDCA-4 (NRP1)	0.479	***	0.431	***	0.305	***	0.298	***	0.146	***	0.207	***
	CD11C (ITGAX)	0.652	***	0.511	***	0.718	***	0.648	***	0.703	***	0.638	***

Table 1: (continued)

Description	Gene markers	SKCM				LUAD				LGG			
		None		Purity		None		Purity		None		Purity	
		cor	p-Value	cor	p-Value	cor	p-Value	cor	p-Value	cor	p-Value	cor	p-Value
Th1	T-bet (TBX21)	0.805	***	0.701	***	0.647	***	0.552	***	0.2	***	0.223	***
	STAT4	0.806	***	0.711	***	0.579	***	0.468	***	−0.121	**	−0.204	***
	STAT1	0.665	***	0.596	***	0.461	***	0.379	***	0.423	***	0.428	***
	IFN-γ (IFNG)	0.733	***	0.612	***	0.449	***	0.342	***	0.278	***	0.245	***
	TNF-α (TNF)	0.665	***	0.512	***	0.49	***	0.363	***	0.348	***	0.304	***
Th2	GATA3	0.712	***	0.528	***	0.573	***	0.47	***	0.418	***	0.371	***
	STAT6	0.105	**	0.173	***	0.184	***	0.232	***	0.576	***	0.479	***
	STAT5A	0.264	***	0.331	***	0.734	***	0.671	***	0.745	***	0.689	***
	IL13	0.197	***	0.108	**	0.194	***	0.103	*	−0.061	0.168	−0.069	0.13
Tfh	BCL6	0.442	***	0.397	***	0.15	***	0.155	***	0.198	***	0.256	***
	IL21	0.58	***	0.474	***	0.375	***	0.32	***	0.092	*	0.092	*
Th17	STAT3	0.381	***	0.401	***	0.186	***	0.228	***	0.524	***	0.567	***
	IL17A	−0.057	0.218	−0.131	**	0.245	***	0.159	***	−0.002	0.96	−0.015	0.74
Treg	FOXP3	0.72	***	0.573	***	0.693	***	0.607	***	−0.145	***	−0.116	*
	CCR8	0.814	***	0.744	***	0.73	***	0.665	***	0.156	***	0.152	***
	STAT5B	0.358	***	0.471	***	0.465	***	0.494	***	0.03	0.492	0.153	***
	TGFB1	0.463	***	0.324	***	0.511	***	0.44	***	0.696	***	0.648	***
T Cell exhaustion	PD-1 (PDCD1)	0.751	***	0.621	***	0.59	***	0.478	***	0.421	***	0.393	***
	CTLA4	0.531	***	0.36	***	0.679	***	0.574	***	0.383	***	0.331	***
	LAG3	0.716	***	0.58	***	0.486	***	0.38	***	0.171	***	0.212	***
	TIM-3 (HAVCR2)	0.858	***	0.791	***	0.787	***	0.731	***	0.898	***	0.876	***
	GZMB	0.707	***	0.535	***	0.433	***	0.305	***	0.142	***	0.171	***

TAM, tumor-associated macrophage; Th, T helper cell; Tfh, Follicular helper T cell; Treg, regulatory T cell; Cor, r value of Spearman's correlation; None, correlation without adjustment. Purity, correlation adjusted by purity. *p<0.01; **p<0.001; ***p<0.0001.

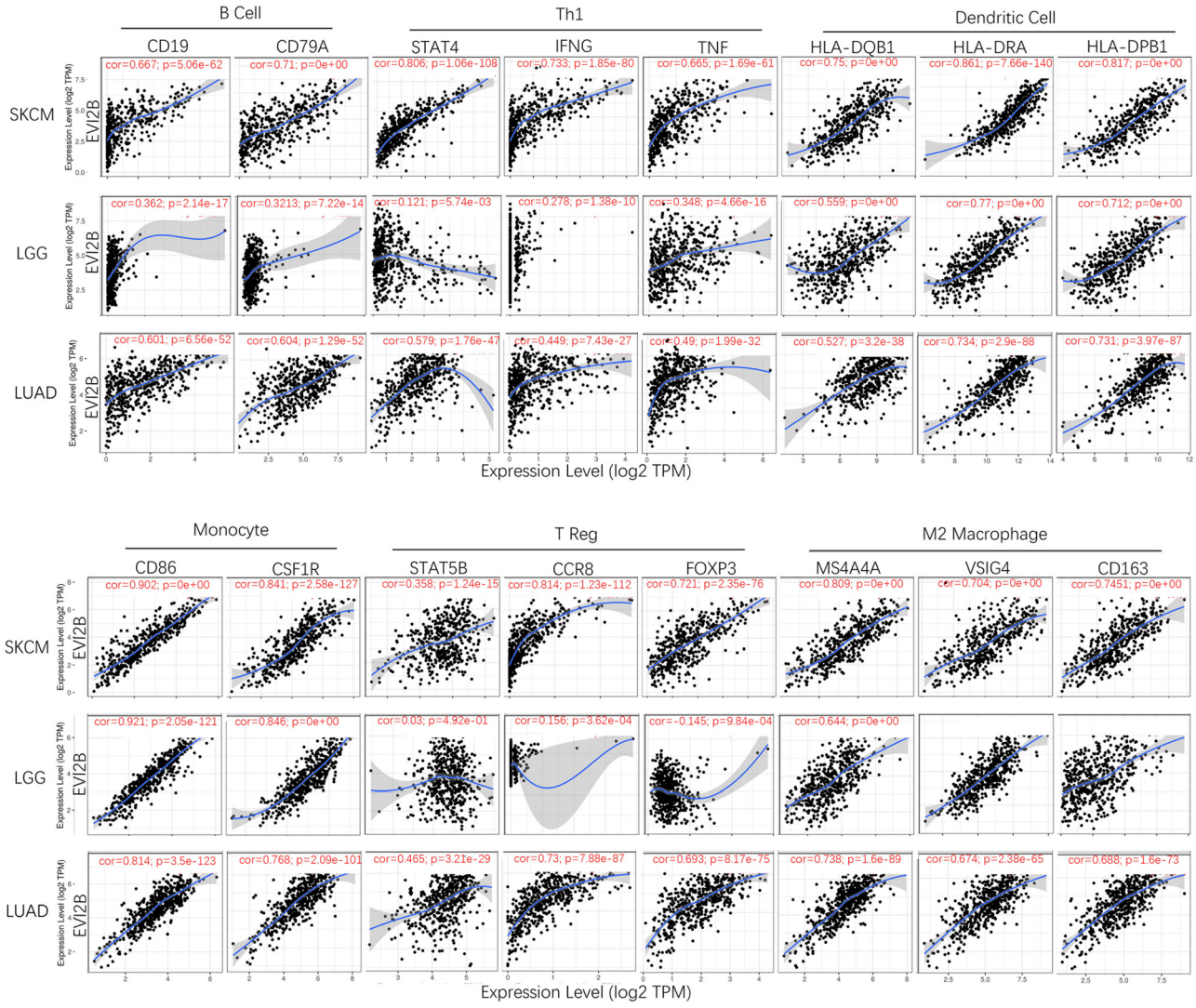

Figure 8: The relationships between *EVI2B*'s expression levels and the marker genes of various tumor-infiltrating anti-tumor immunocyte types, i.e. monocytes, B cells, dendritic cells, T cells, M2 macrophages, and Th1 cells. Scattered dots show the relationship between *EVI2B*'s and immunocytes marker genes' expression levels. Each dot stands for a clinical sample. LGG (n=505); LUAD (n=482); SKCM (n=425). The blue continuous line means the average expression of *EVI2B* at each level. The R value of correlation analysis and p value for *t*-test are presented in red. The R>0 and p<0.05 represent the statistically significant positive relationship between *EVI2B* and immune markers.

the immunocytes are regarded as a double-edged sword [22]. On one hand, the immunocytes can promote tumorigenesis. For instance, specific immunocytes, such as tumor-associated macrophages, engage in angiogenesis, invasion, and metastasis. Moreover, immune cell-mediated inflammation is an important tumor-promoting factor when several non-mutagenic factors are involved, such as in LUAD cases driven by asbestos or silica particles [23].

On the other hand, some immune cell types, such as T cytotoxic cells and T helper (Th) cells, were associated with longer-lasting patients' survival in melanoma, colon cancer, and pancreatic cancer [24–26]. Our results showed that an upregulated *EVI2B*'s expression correlated with tumor progression heterogeneity in LGG, LUAD, and SKCM. However, distinct mechanisms of the EVI2B-mediated signaling pathways contribute to divergent immune responses in different types of cancer. Our results suggest that an elevated *EVI2B*'s expression is associated with longer survival rates in LUAD and SKCM, but with a poorer prognosis in LGG. Notably, the expression levels of most immunological markers of $CD8^+$ T cells, Tregs, Th1, and Tfh cells showed a strong positive relationship with *EVI2B*'s expression in LUAD and SKCM but not in LGG. These findings revealed that EVI2B promoted a more intense infiltration of $CD8^+$ T cells in LUAD and SKCM than in LGG. Conversely, EVI2B promoted more $CD4^+$ T cells and

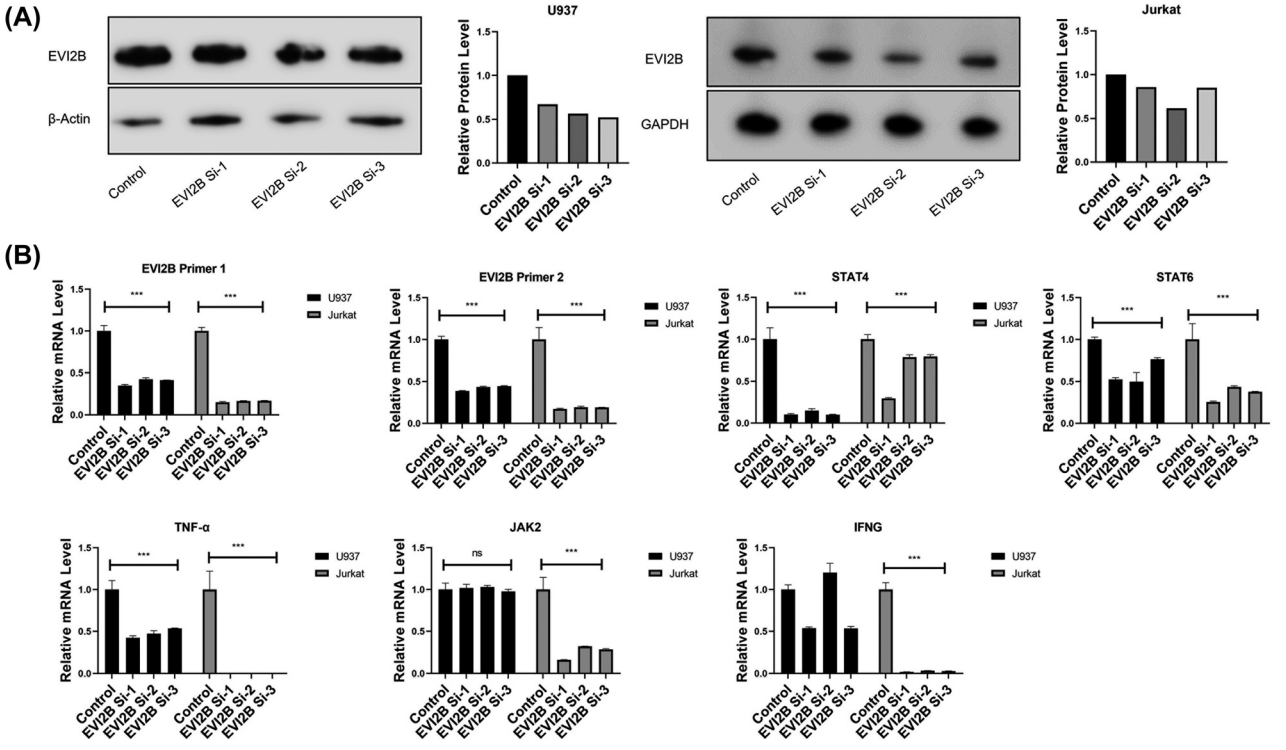

Figure 9: EVI2B protein knock-down validation in U937 and JURKAT immune cell lines and its effects on the mRNA expression of genes related to JAK-STAT, TNF-α, and IFN-γ signaling pathways. (A) Western immunoblotting for EVI2B protein levels in the silenced U937 and Jurkat cell lines, respectively. (B) RT-PCR analysis of the tumor-infiltrating immunocytes-related pathways. The significance was evaluated via *t*-test. p<0.05: *, p<0.01: **, p < 0.005: ***.

macrophage infiltration in LGG than in the other two malignancies (Figure 10A).

Since Th cells constitute a significant group of the $CD4^+$ T cells, and because Th cells can be classified into Th1 and Th2 cells, we investigated the tumor-infiltrating Th cell subtypes. In LUAD and SKCM, a positive correlation existed between an increased Th1 cell infiltration and *EVI2B* expression, while the infiltration of Th2 cells was more evident in LGG. As the immune system functions, in most cases a higher level of $CD8^+$ T cell infiltration associates with an increased survival rate. In contrast, a high level of macrophages infiltration is coupled with poorer clinical outcomes [27]. Various studies have proven that Th1 function as antitumor cells while Th2 act as tumor promoting cells [28]. Our findings suggest that an increased *EVI2B*'s expression modulated patients' prognosis not only by differently influencing cell proliferation according to the specific tumor type but also through divergently regulating the specific tumor-infiltrating immunocytes. The integration of these two EVI2B mechanisms of action helped advance the survival of LUAD and SKCM patients while accelerating the demise of LGG's patients (Figure 10A).

Furthermore, we investigated the molecular mechanisms by which EVI2B impacts tumor-infiltrating immunocytes. We grouped the LUAD, LGG, and SKCM patients based on the *EVI2B*'s expression levels and analyzed the DEGs of the high- and low- *EVI2B*-expression groups. Notably, the activation of JAK-STAT pathway occurred in all three types of cancers. The JAK-STAT pathway is a critical axis in tumor immunology [29]. The extracellular Interleukins (ILs) and interferons (IFNs) can activate the JAK-STAT kinase system and the downstream NF-κB pathway and other transcriptional processes [30]. The STAT family encompasses seven members, i.e. STATs 1–4, 5A, 5B, and 6 [31]. When this signaling pathway is activated, the STAT proteins play an oncogenic or antioncogenic role depending upon the upstream signaling molecules and the targeted tumor-infiltrating immune cell types. In this study, we saw the upregulation of STAT5 in all three types of cancers examined, i.e., LUAD, SKCM, and LGG. In a tumor microenvironment, an activated STAT5 in NK cells would promote IFN-γ's secretion and play an antioncogenic role [32]. In Th cells and Treg cells, activated STAT5 would drive the production of ILs playing oncogenic roles [33]. On this basis, we posit that the different effects elicited by STAT5 underlie the shorter survival of LGG patients compared to that of LUAD and SKCM. Our view is strengthened by the observed upregulation of the

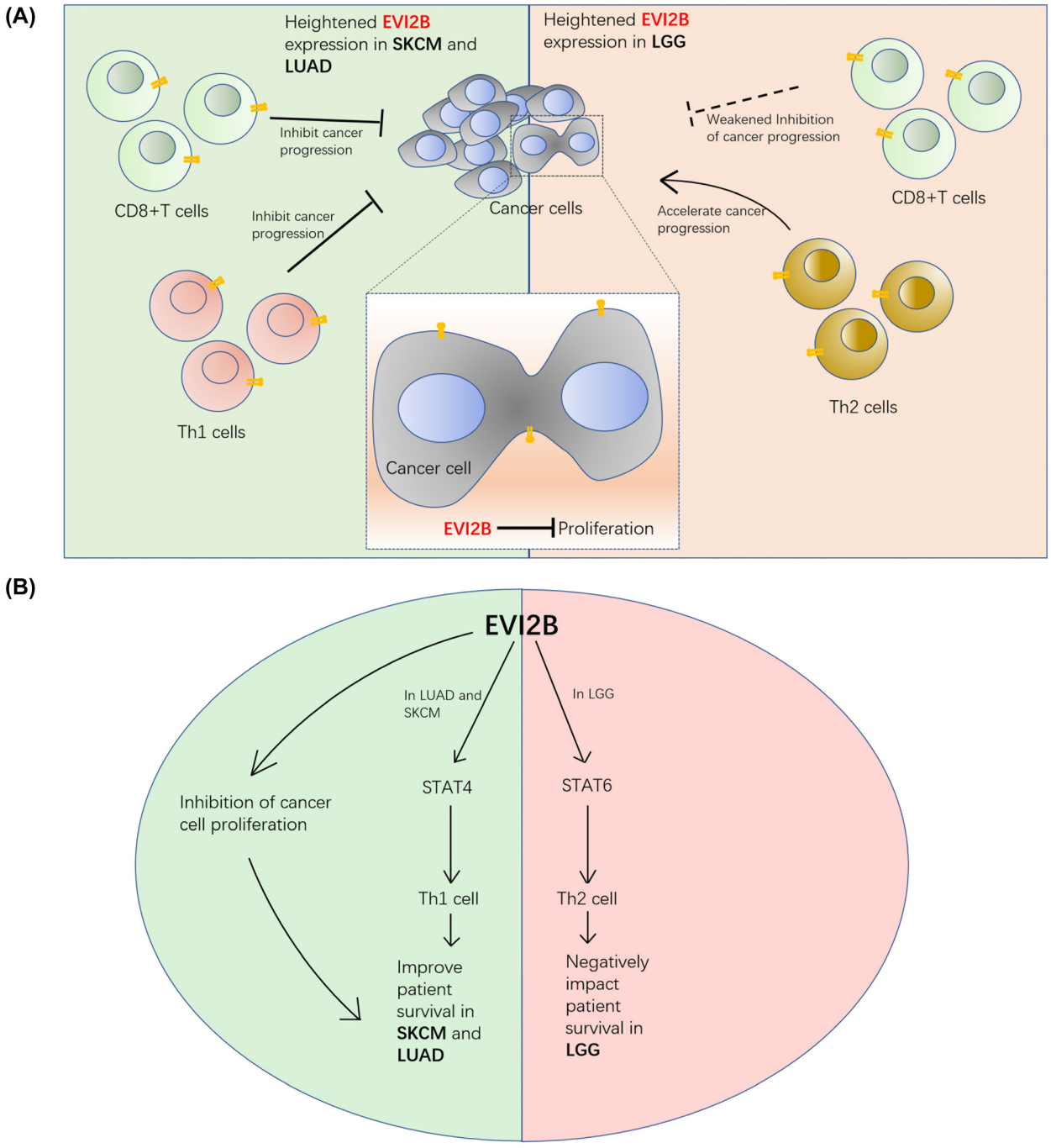

Figure 10: Cellular mechanism and molecular interaction of EVI2B in cancer progression. (A) The Janus-faced regulation mechanism of EVI2B in different types of cancers. EVI2B inhibits the cell proliferation in various types of cancer cells including SKCM, LUAD and LGG. In SKCM and LUAD, the heightened *EVI2B* expression activates the anti-cancer immune cells ($CD8^+$ T cells and Th1 cells) to inhibit the cancer progression. On the contrary, in LGG, the high EVI2B level triggers strong pro-cancer immune cell response and diminishes the anti-cancer cell response of $CD8^+$ T. (B) *EVI2B* acts as a janus-faced oncogene/antioncogene by differently activating the downstream target genes. In SKCM and LUAD, *EVI2B* activates STAT4 and Th1 cells acted as an antioncogene. Conversely, in LGG, *EVI2B* activates STAT6 and Th2 cells acted as an oncogene.

proinflammatory and antioncogenic IFN-γ that occurred only in LUAD and SKCM. Conversely, IFN-γ was downregulated in LGG with pro-oncogenic consequences concurring with *EVI2B*'s high expression. The direct, whether pro-oncogenic or antioncogenic, the effect of EVI2B on LGG cells remains to be determined.

Besides, STAT5 and STAT6 are the biomarkers of the Th2 cell, which is a type of tumor promoting $CD4^+$ immune cell [34]. Notably, IL-4 drives native $CD4^+$ cells to highly express STAT6 and GATA3 and next to differentiate into Th2 cells. When activated by STAT5 and STAT6, Th2 cells start a self-activating positive feedback cycle entailing further IL-4 secretion. Concurrently, pro-oncogenic Th2 cells can suppress antioncogenic Th1 cells [35–37]. Consistently, our results showed that Th2 cell numbers were significantly lower in LGG than in LUAD and SKCM (Figure 10B).

In summary, in LGG *EVI2B*'s expression promoted the infiltration of pro-oncogenic Th2 cells while suppressing that of the anti-oncogenic Th1 cells. Conversely, *EVI2B*'s expression advanced the antitumor Th1 cells' infiltration in both SKCM and LUAD. Besides, EVI2B could upregulate STAT4, which is critical in promoting the infiltration of in most antitumor immunocytes, such as Th1 cells, NK cells, and $CD8^+$ T cells [38]. A main factor underlying the two different prognoses of the types of cancer examined could be that EVI2B activated STAT4 in SKCM and LUAD but did not do it in LGG.

EVI2B's inhibitory effect on cell proliferation in various cancer cell lines implies that the eventual prognostic regulation of EVI2B is due to the integration of its intracellular and extracellular effects.

Altered DNA methylation patterns are a typical feature of oncogenesis as the fast-proliferating neoplastic cells require a more dynamic transcriptional activity. Hence, their genome has low levels of methylation [39]. Consistent with this, an increased *EVI2B*'s expression was associated with genomic demethylation in LGG, while the opposite occurred in SKCM and LUAD. Leaving aside variations in global DNA methylation levels, we found that the expression of JAK-STAT pathway's genes diverged according to their methylation. STAT6 was demethylated when *EVI2B* was highly expressed in LGG. This could have driven STAT6's strong upregulation in LGG, which did not occur in SKCM and LUAD. To date, only few studies have investigated the molecular pathways EVI2B affects in oncogenesis. Even though our data linked heightened *EVI2B* expression levels with a decreased genomic methylation in LGG, the clarification of the detailed molecular mechanism(s) through which EVI2B regulated this process in different cancerous growths remains the target of further studies.

Conclusions

Altogether, the present study's prognostic, transcriptomic, and methylomic data offer comprehensive evidence that EVI2B is a double-faced oncogene/antioncogene affecting both directly via neoplastic cells growth and indirectly via the specific induction of pro- or anti-tumor-infiltrating immunocytes-neoplastic cells growth rates according to tumor-specific patterns. These findings warrant further in-depth studies on EVI2B's intracellular and extracellular effects on a broader range of human tumors.

Research funding: This research was supported by National Natural Science Foundation of China (82172214, 82002936), Natural Science Foundation of Guangdong Province, China (2020A1515010613), Provincial key clinical specialty-burn surgery (2000004), Shenzhen Science and Technology Innovation Committee JCYJ20190806163209126, The Key Basic Research Project of Shenzhen Science and Technology Program (JCYJ20200109115635440), Retired Expert Program of Guangdong Province (202020031911500002), and Shenzhen-Hong Kong-Macau Technology Research Programme (Type C: SGDX2020110309300301).

Author contributions: Fangyingnan Zhang and Xinning Wang executed the experiments and analyzed the data. Fangyingnan Zhang and Jun Wu conceived the project design. Fangyingnan Zhang, Saquib Waheed, Ubaldo Armato, Ilaria Dal Prà, Anna Chiarini, Zhibin Li, and Xinning Wang co-wrote the manuscript. Chao Zhang, Jun Wu, and Zhibin Li supervised the work. All authors contributed to the discussion of results and commented on the final manuscript. All authors have accepted responsibility for the entire content of this manuscript and approved its submission.

Competing interests: Authors state no conflict of interest.

Informed consent: Not applicable.

Ethical approval: The Ethical Committee of the First Affiliated Hospital of Shenzhen University approved this research on 2021-06-18. The ethical code number is 20210615008.

References

1. Anne C, Elisabeth Q, Norman W, David S, Gabrielle P, Harvey K. The increasing incidence of lung adenocarcinoma: reality or artefact? A review of the epidemiology of lung adenocarcinoma. Int J Epidemiol 1997;26:14–23.
2. Bray F, Ferlay J, Soerjomataram I, Siegel RL, Torre LA, Jemal A. Global cancer statistics 2018: GLOBOCAN estimates of incidence and mortality worldwide for 36 cancers in 185 countries. CA Cancer J Clin 2018;68: 394–424.
3. Quinn O, Haley G, Gabrielle T, Alexander B, Carol K, Jill SB. CBTRUS statistical report: primary brain and other central nervous system tumors diagnosed in the United States in 2011-2015. Neuro Oncol 2018; 20:1–86.
4. Johan P, Marie B, Emmanuel M, Etienne A, Denys F, Nader S, et al. Velocity of tumor spontaneous expansion predicts long-term outcomes for diffuse low-grade gliomas. Neuro Oncol 2013;15:595–606.

5. Patrick W, Santosh K. Malignant gliomas in adults. New Engl J Med 2008;359:492–507.
6. Moriah HN, Christine AP, Alexis MJ, Ricardo R, Helen W, Cailian L, et al. Loss of NF1 in cutaneous melanoma is associated with RAS activation and MEK dependence. Cancer Res 2014;74:2340–50.
7. Dirk S, Alexander A, Carola B, Klaus G, Ralf G, Axel H, et al. Melanoma. Lancet 2018;392:971–84.
8. Dieter K, Susanne G, Friederike B, Markus S, Johann G, Sven H, et al. EVI2B, a gene lying in an intron of the neurofibromatosis type 1 (NF1) gene, is as the NF1 gene involved in differentiation of melanocytes and keratinocytes and is overexpressed in cells derived from NF1 neurofibromas. DNA Cell Biol 1999;18:345–56.
9. Polina Z, Miroslava K, Petr D, Pavla A, Touati B, Alexander AW, et al. EVI2B is a C/EBPalpha target gene required for granulocytic differentiation and functionality of hematopoietic progenitors. Cell Death Differ 2017;24:705–16.
10. Bingsheng Y, Zexin S, Guoli C, Zhirui Z, Jianye T, Guofeng W, et al. Identification of prognostic biomarkers associated with metastasis and immune infiltration in osteosarcoma. Oncol Lett 2021;21:180.
11. Mingyii H, Hweiming W, Teck-Siang T, Huijen C, Mingsung C, Tianlu C, et al. EVI2B, ATP2A2, S100B, TM4SF3, and OLFM4 as potential prognostic markers for postoperative Taiwanese colorectal cancer patients. DNA Cell Biol 2012;31:625–35.
12. Satoru Y, Kosuke U. EVI2B Is a new prognostic biomarker in metastatic melanoma with IFN gamma associated immune infiltration. Cancers 2021;13:4110.
13. Wanwan L, Michael K. A cytokine-mediated link between innate immunity, inflammation, and cancer. J Clin Invest 2007;117:1175–83.
14. Rajesh S, Manoj K, Himanshu A. Immunity, inflammation, and cancer. Cell 2010;140:883–99.
15. Borros A. Tumor microenvironment. Medicina (Kaunas) 2019;56:15.
16. Andrew DK, Karthikeyan M, Zheng K, Meagan M, Jeffrey SR, Lee A, et al. Pan-cancer landscape of CD274 (PD-L1) rearrangements in 283,050 patient samples, its correlation with PD-L1 protein expression, and immunotherapy response. J Immunother Cancer 2021;9:e003550.
17. Zefang T, Chenwei L, Boxi K, Ge G, Cheng L, Zemin Z. GEPIA: a web server for cancer and normal gene expression profiling and interactive analyses. Nucleic Acids Res 2017;45:98–102.
18. Ethan C, Jianjiong G, Ugur D, Benjamin EG, Selcuk OS, Bülent AA, et al. The cBio cancer genomics portal: an open platform for exploring multidimensional cancer genomics data. Cancer Discov 2012;2:401–4.
19. Dawei H, Brad TS, Qina T, Joseph K, David L, David B. DAVID Bioinformatics Resources: expanded annotation database and novel algorithms to better extract biology from large gene lists. Nucleic Acids Res 2007;35:169–75.
20. Bo L, Eric S, Jean-Christophe P, Haoquan Z, Taiwen L, Jesse N, et al. Comprehensive analyses of tumor immunity: implications for cancer immunotherapy. Genome Biol 2016; 22:174.
21. Thomas FG, Hans S, Yangxin F. Innate and adaptive immune cells in the tumor microenvironment. Nat Immunol 2013;14:1014–22.
22. Seila LH, Christian SB, Segundo G, Alejandro LS. Immunosurveillance of cancer cell stress. Cell Stress 2019;3:295–309.
23. Catherine D, Virginie P, Robin VB, Chad S, Brooke TM, Jürg T. Innate immune activation through Nalp3 inflammasome sensing of asbestos and silica. Science 2008; 320:674–7.
24. Luigi L, Paolo B, Elena M, Emanuela B, Veronica P, Fabio G, et al. CD3+ cells at the invasive margin of deeply invading (pT3-T4) colorectal cancer and risk of post-surgical metastasis: a longitudinal study. Lancet Oncol 2009;10:877–84.
25. Jérôme G, Anne C, Fatima SC, Amos K, Bernhard M, Christine LP, et al. Type, density, and location of immune cells within human colorectal tumors predict clinical outcome. Science 2006;313:1960–4.
26. Jeremy BS, Mark JS. Immune surveillance of tumors. J Clin Invest 2007; 117:1137–46.
27. Nomathamsanqa RM, Shasha L, Yi Z. Fates of CD8+ T cells in tumor microenvironment. Comput Struct Biotechnol J 2018;17:1–13.
28. Contact K, Disis M. Tumor antigen-specific T helper cells in cancer immunity and immunotherapy. Cancer Immunol Immunother 2005; 54:721–8.
29. Bernd G, Viktoria M. Jak Stat signaling and cancer: opportunities, benefits and side effects of targeted inhibition. Mol Cell Endocrinol 2017;451:1–14.
30. Katie LO, Natasha KB, Belinda SP. JAK-STAT signaling: a double-edged sword of immune regulation and cancer progression. Cancers 2019;11: 2002.
31. Farhad S, Majid K, Hossein A, Monireh M, Gholamreza S, Mohammadali B. The role of JAK-STAT signaling pathway and its regulators in the fate of T helper cells. Cell Commun Signal 2017;15:23.
32. Grégory V, Toby L, Anne MS, Nathalie AA. Targeting STAT3 and STAT5 in tumor-associated immune cells to improve immunotherapy. Cancers 2019;11:1832.
33. Aradhana R, John JM. STAT5 in cancer and immunity. J Interferon Cytokine Res 2016;36:226–37.
34. Paul WE. Interleukin 4: signalling mechanisms and control of T cell differentiation. Ciba Found Symp 1997;204:208–16.
35. Yuan Z, Yaguang Z, Wangpeng G, Bing S. TH1/TH2 cell differentiation and molecular signals. Adv Exp Med Biol 2014;841:15–44.
36. Parris K. Th1/Th2 balance: the hypothesis, its limitations, and implications for health and disease. Altern Med Rev 2003;8:223–46.
37. Yuan Z, Yaguang Z, Wangpeng G, Lan H, Bing S. Th1/Th2 cell's function in immune system. Adv Exp Med Biol 2014;841:45–65.
38. Andrea LW, Takashi T, Michael JG. The biology of Stat4 and Stat6. Oncogene 2000;19:2577–84.
39. Yunbao P, Guohong L, Fuling Z, Bojin S, Yirong L. DNA methylation profiles in cancer diagnosis and therapeutics. Clin Exp Med 2018;18: 1–14.

Supplementary Material: This article contains supplementary material (https://doi.org/10.1515/oncologie-2022-1002).